Honeybee Iflaviruses Pack Specific tRNA Fragments from Host Cells in Their Virions

Anna Šimonová,[a, b] Veronika Romanská,[a] Barbora Benoni,[a, b] Karel Škubník,[c] Lenka Šmerdová,[c] Michaela Procházková,[c] Kristina Spustová,[a] Ondřej Moravčík,[d] Lenka Gahurova,[a, e] Jan Pačes,[d, f] Pavel Plevka,[c] and Hana Cahová*[a]

The *Picornavirales* include viruses that infect vertebrates, insects, and plants. It was believed that they pack only their genomic mRNA in the particles; thus, we envisaged these viruses as excellent model systems for studies of mRNA modifications. We used LC–MS to analyze digested RNA isolated from particles of the sacbrood and deformed wing iflaviruses as well as of the echovirus 18 and rhinovirus 2 picornaviruses. Whereas in the picornavirus RNAs we detected only N^6-methyladenosine and 2′-*O*-methylated nucleosides, the iflavirus RNAs contained a wide range of methylated nucleosides, such as 1-methyladenosine (m^1A) and 5-methylcytidine (m^5C). Mapping of m^1A and m^5C through RNA sequencing of the SBV and DWV RNAs revealed the presence of tRNA molecules. Both modifications were detected only in tRNA. Further analysis revealed that tRNAs are present in form of 3′ and 5′ fragments and they are packed selectively. Moreover, these tRNAs are typically packed by other viruses.

Introduction

More than 170 RNA modifications are currently known to be naturally present in various types of RNA.[1] They are the best studied in the abundant RNA moieties such as tRNA and rRNA. The discovery of the N^6-methyladenosine (m^6A) in mRNA[2] represents a milestone in the field and triggered a new search for other modifications in coding RNA such as mRNA or viral genomic RNA. The detection of RNA modifications in mRNA is still limited by the amount and purity of the mRNA. The contamination of mRNA by tRNA and rRNA causes false positive LC–MS detection of RNA modifications coming from these abundant RNA species. Alternative detection techniques selective to particular RNA modification are combined with RNA sequencing (RNA-seq) and bring information on exact position of the modification in the RNA sequence. Nevertheless, some methods suffer from false positive output as well. Typical example is interaction of modification specific antibodies with unmodified parts of RNA.[3] Another example can be false positive detection of m^5C in highly structured RNA such as viroids.[4] Therefore, it is necessary to combine various techniques to prove the presence of certain RNA modifications in low abundant species.[5] While m^6A is an indisputable marker on coding RNA with significant impact on RNA stability and recognition proteins as the writers, erasers and readers are known, the roles and mechanisms of action for other RNA modifications should be still revealed. So far, only m^6A, m^5C, Inosine (I) and 2′-*O*-methyl (Nm) were discovered and confirmed as part of various viral genomic or viral encoded mRNA.[6]

In our search for viral mRNA modifications, we focused on various representatives from insect and human *Picornavirales* (sacbrood virus (SBV), deformed wing virus (DWV), human rhinovirus-2 (RV2) and Echovirus 18 (E18)) as model systems to reveal RNA modifications in their genomic RNA. Until now, only m^6A was reported to be present in RNA from picornavirus enterovirus 71.[7] It was shown that the presence of m^6A in two positions of genomic viral RNA positively modulated viral replication.

The family *Picornaviridae* includes viruses that infect vertebrates and cause numerous diseases in humans. The illnesses caused by picornaviruses range from mild upper and lower respiratory tract infections, gastroenteritis, hepargina, hand-foot-and-mouth-disease to life-threatening encephalitis.[8] Human rhinoviruses, including rhinovirus 2 (RV2) are responsible

[a] A. Šimonová, V. Romanská, B. Benoni, K. Spustová, Dr. L. Gahurova, Dr. H. Cahová
Institute of Organic Chemistry and Biochemistry of the Czech Academy of Sciences
Flemingovo nam. 2, 16610 Prague 6 (Czech Republic)
E-mail: cahova@uochb.cas.cz
[b] A. Šimonová, B. Benoni
First Faculty of Medicine Charles University
Katerinská 32, 12108 Prague 2 (Czech Republic)
[c] Dr. K. Škubník, Dr. L. Šmerdová, M. Procházková, Dr. P. Plevka
Structural Virology, Central European Institute of Technology
Masaryk University, Kamenice 753/5, 62500 Brno (Czech Republic)
[d] O. Moravčík, Dr. J. Pačes
Institute of Molecular Genetics of the Czech Academy of Sciences
14220 Prague (Czech Republic)
[e] Dr. L. Gahurova
Department of Molecular Biology and Genetics
Faculty of Science, University of South Bohemia
Branisovska 1760, 37005 České Budějovice (Czech Republic)
[f] Dr. J. Pačes
University of Chemistry and Technology
16628 Prague (Czech Republic)

Supporting information for this article is available on the WWW under https://doi.org/10.1002/cbic.202200281

This article is part of the Special Collection ChemBioTalents2022. Please see our homepage for more articles in the collection.

© 2022 The Authors. ChemBioChem published by Wiley-VCH GmbH. This is an open access article under the terms of the Creative Commons Attribution Non-Commercial License, which permits use, distribution and reproduction in any medium, provided the original work is properly cited and is not used for commercial purposes.

© 2022 The Authors. ChemBioChem published by Wiley-VCH GmbH

for 40% of the common cold cases that result in yearly cost of about $16 billion in treatments and lost working hours within the United States alone.[8] Echovirus 18, an enterovirus from the family *Picornaviridae*, causes aseptic meningitis and exanthema in humans.[9]

Apart from human viruses, the most important honeybee viruses also belong to the order *Picornavirale*, particularly the family *Iflaviridae*: deformed wing virus (DWV) and sacbrood virus (SBV).[10] Honeybee (*Apis mellifera*) is found all over the world and plays a vital role in agricultural industry by providing pollination services for many food crops. However, the virus infections are one of the major threats to the health and productivity of the honeybee colonies.[11]

For our study, we selected *Picornavirales* as their RNA serves as both the genomic and mRNA and their virions should contain only viral RNA. Therefore, the RNA purified from the particle should not be contaminated by the otherwise abundant host tRNA and rRNA,[12] as it is common for cellular mRNA or for viral RNA isolated from retroviruses such as HIV-1.[13] Thus, this work should answer the basic question: what are the typical RNA modifications in mRNA.

In this work, we isolated RNA from pure virions and we digested it into form of nucleosides. The digested mixtures were then analyzed using LC–MS and compared with standard modified nucleosides. While we observed only 2′-O-methylated nucleosides in RNA isolated from human picornaviruses (RV2, E18), the RNA isolated from insect viruses (SBV and DWV) contained significant amount of other methylated nucleosides e.g. 1-methyladenosine (m^1A) or m^5C. Therefore, we applied two profiling techniques in combination with RNA-seq to map m^1A and m^5C in the viral RNA isolated from iflaviruses. The bioinformatic analysis of these RNA-seq libraries did not confirm m^1A and m^5C in the viral genomic RNA. Nevertheless, we detected specific honeybee tRNAs,[14] which were co-packed in the virions together with viral genomic RNA. Surprisingly, we observed only specific tRNAs such as various isoforms of $tRNA^{LysTTT}$, $tRNA^{LysCTT}$, $tRNA^{GlyGCC}$ or $tRNA^{AspGTC}$. We compared this finding with a codon usage of the host organism – honeybee. With exception of Lys AAA codon, other do not belong among the most used tRNAs in the host organism. Moreover, these particular types of tRNA are also the most abundant in HIV-1 virions,[13a–c] what suggests their general role in virus life cycle.

Hana received her PhD at UCT Prague and IOCB Prague in organic chemistry under the supervision of Prof. Michal Hocek. In 2011, she was awarded the Humboldt Research Fellowship and she joined Prof. Andres Jäschke's laboratory at Heidelberg University. As postdoctoral fellow, she worked on photoswitchable DNA and she developed NAD captureSeq for identification of NAD-RNA. She has been the head of the Junior Research Group of Chemical Biology at IOCB Prague since 2016. Together with her team she focuses on understanding the role of RNA modifications in viruses and other model organisms.

Nevertheless, the Northern blot analysis showed the presence of 3′ and 5′ tRNA fragments with length around 20 nt in viral particles, while the whole tRNAs were observed only in bee RNA.

Results

LC–MS analysis of RNA from virions

Virions of E18, RV2, SBV, and DWV were purified using CsCl gradient. The purity of the virions was confirmed using cryo-electron micrographs. Before RNA isolation from viral particles, any unpacked RNA or DNA was digested by RNase and DNase treatment (Figure SI1). In the next step, the isolated RNA was digested by Nuclease P1 and Alkaline phosphatase into form of nucleosides and analyzed by LC–MS method (Figure 1a, Figure SI 2). The LC–MS analyses of the digested RNA from insect SBV, DWV and human RV2 and E18 were compared with common methylated nucleoside standards (1-methyladenosine (m^1A), N^6-methyladenosine (m^6A), 2′-*O*-methyladenosine (Am), 1-methylguanosine (m^1G), 2-methylguanosine (m^2G), N^7-methylguanosine (m^7G), 2′-*O*-methylguanosine (Gm), 3-methylcytidine (m^3C), 5-methylcytidine (m^5C), 2′-*O*-methylcytidine (Cm), 5-methyluridine (m^5U) and 2′-*O*-methyluridine (Um)) (Table SI 1, Figure SI 3, 4). The 2′-*O*-methylated nucleosides are known to be present in mRNA in general[15] and we identified them almost in all samples. Also, the detection of m^6A in viral RNA was expected.[7] While human viruses did not contain any significant numbers of other methylated nucleotides, surprisingly, we identified substantial amount of various methylated nucleosides (m^1A, m^1G, m^2G, m^7G, m^5C etc.) rather typical for tRNAs in RNA isolated from iflaviruses (Figure 1b, Figures SI 5–8).

RNA-seq for RNA modifications detection

The detected methylated nucleosides can come either from viral genomic RNA or from co-packed host RNA. Even though the co-packing of host RNA in the *Picornavirales* virions has not been reported yet, we also considered this option. To answer this question, we prepared RNA sequencing (RNA-seq) libraries with focus on m^1A (SBV) and m^5C (SBV, DWV) profiling. The m^1A modification was detected by the method used recently for identification of m^1A positions in the RNA of HIV-1 viral particle.[13a] As m^1A disturbs Watson-Crick base-pairing, it causes problems to reverse transcriptase in recognition and thus misincorporation or breaks can be observed in bioinformatic data. As a control we converted m^1A to m^6A by Dimroth rearrangement (alkali conditions) (Figure 2a). We used two types of reverse transcriptases (Superscript III, TGIRT) for m^1A position confirmation.[16] The m^1A position was then bioinformatically detected by misincorporation pattern (less prominent in the control samples after alkaline treatment). The m^5C was detected by optimized bisulfite sequencing method (Figure 2a).

© 2022 The Authors. ChemBioChem published by Wiley-VCH GmbH

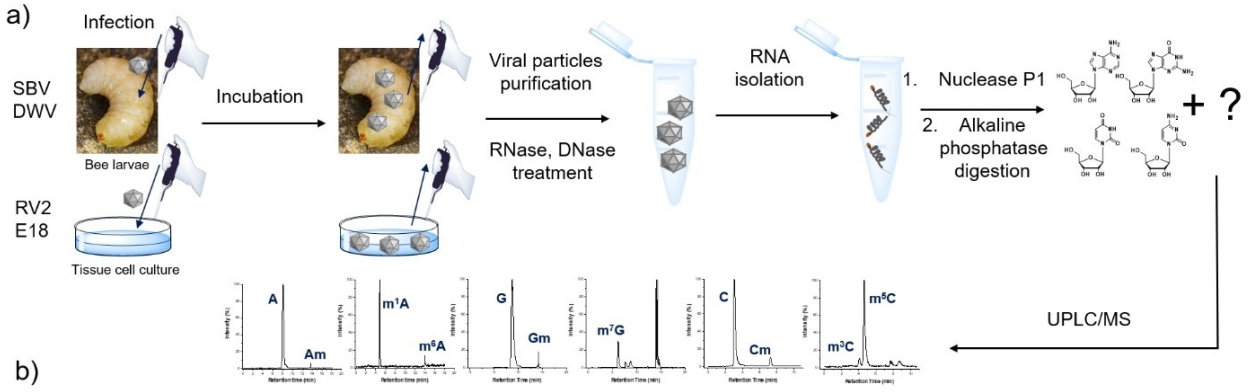

	Genome length (nt)	m¹A/100A	m⁶A/100A	Am/100A	m¹G/100G	m²G/100G	m⁷G/100G	Gm/100G	m³C/100C	m⁵C/100C	Cm/100C	ψ/100U	m⁵U/100U	Um/100U
SBV	8832	0.06 ± 0.02	0.01 ± 0.01	0.18 ± 0.12	0.08 ± 0.03	0.22 ± 0.08	0.19 ± 0.04	0.66 ± 0.31	0.03 ± 0.04	0.28 ± 0.13	1.00 ± 0.60	0.00	0.03 ± 0.04	0.36 ± 0.32
DWV	10071	0.37 ± 0.01	0.06 ± 0.01	0.95 ± 0.06	0.53 ± 0.02	1.32 ± 0.07	0.99 ± 0.01	2.43 ± 0.19	0.16 ± 0.02	1.44 ± 0.02	3.67 ± 1.09	0.00	0.60 ± 0.01	1.75 ± 0.16
RV2	7120	0.01 ± 0.01	0.05 ± 0.06	0.20 ± 0.07	0.01 ± 0.01	0.03 ± 0.01	0.04 ± 0.04	0.90 ± 1.14	0.00	0.00	0.14 ± 0.17	0.00	0.00	0.00
E18	7410	0.00	0.00	0.12 ± 0.07	0.00	0.02 ± 0.03	0.00	0.00	0.00	0.00	0.00	0.00	0.00	0.00

Number of mod. nucleoside per 100 of unmodified: 0-0.05 | 0.05-0.2 | 0.2-1 | 1-4

Figure 1. LC–MS analysis of RNA isolated from virions of insects Iflaviruses (SBV, DWV) and human Picornaviruses (RV2, E18). a) Scheme of workflow. b) Table with detected modified nucleosides per 100 unmodified for every virus. The shade of blue indicates the amount of detected methylated nucleoside.

The bioinformatic analysis revealed the presence of various types of host tRNA in the RNA isolated from virions of SBV and DWV. Surprisingly, the detected tRNAs correspond only partially to those, used by host organism the most. We identified mainly three types of tRNAs: $tRNA^{GlyGCC-1}$, $tRNA^{AspGTC}$ and $tRNA^{LysTTT}$ in both viruses and also $tRNA^{LysCTT}$ in SBV (Figure 2b, c) and $tRNA^{GluCTC}$ in DWV. Apart from these four tRNAs also other types were present in both viruses (Table SI 2). The m^1A profiling technique allowed us to confirm m^1A in some of the detected tRNAs e.g. in position 59 of $tRNA^{LysCTT}$ and position 56 of $tRNA^{GlyGCC-1}$ (Figures SI 9, 10). The disappearance of the base misincorporation (A for T) after alkali treatment was detected in experiments with both or at least one reverse transcriptase. Even though, we detected the misincorporations (base mismatch) of A in other tRNAs in otherwise typical positions for m^1A (8 and 10 in $tRNA^{AspGTC}$ or 59 $tRNA^{LysTTT}$), we did not observe the disappearance of the signal after alkali treatment (Figures SI 10, 11). Thus, we concluded that other types of modifications must be present in these positions. The searching for this pattern (base mismatch at A position and disappearance after alkali treatment) in the genomic RNA of SBV did not convincingly show the presence of m^1A in SBV genomic RNA (Table SI 8, Figure SI 13).

The bisulfite sequencing confirmed the presence of various tRNAs in the RNA isolated from virions of SBV and DWV as well. 5-methylcytidine was detected through bisulfite sequencing in some of the most abundant tRNAs co-packed by SBV such as $tRNA^{AspGTC}$ or co-packed by DWV $tRNA^{AspGTC}$, $tRNA^{LysTTT}$ and $tRNA^{GluCTC}$ (Tables SI 3, 4). 5-methylcytidne was usually observed in specific positions in 100% of reads of these tRNAs. Even though, we observed partial conversion of some C to U in genomic RNA from samples treated by bisulfite, we presume that this is caused rather by incomplete bisulfite reaction than by the presence of m^5C in these positions (Table SI 5, 6). Only around 6–7% of C in the particular positions were not converted to U.

Both sequencing experiments lead us to conclusion that m^1A, m^5C and other methylated nucleotides come from the co-packed tRNAs. To support this hypothesis, we also searched for three types of modified adenosines that are typical for eukaryotic tRNAs in general:[17] N^6-threonylcarbamoyladenosine (t^6A), 2-methylthio-N^6-threonylcarbamoyladenosine (ms^2t^6A) and N^6-isopentenyladenosine (i^6A). These modifications are usually present close to anticodon loop and cause the reverse transcription falling i.e. coverage drop in RNA-seq data. The coverage drops were observed for all the detected tRNAs (Figures SI 9–12). In our LC–MS analysis of digested RNA isolated from virions, we compared our samples with LC–MS properties (detected mass and retention time) of standard t^6A and with calculated mass of second two nucleosides (ms^2t^6A and i^6A). We indeed observed these modified nucleosides in RNA isolated from SBV and DWV virions and not in human representative of *Picornavirales* RV2 and E18 (Table SI 7). This observation again confirms our finding that insects *Picornavirales* co-pack specific tRNAs in their virions, while two studied human viruses do not.

© 2022 The Authors. ChemBioChem published by Wiley-VCH GmbH

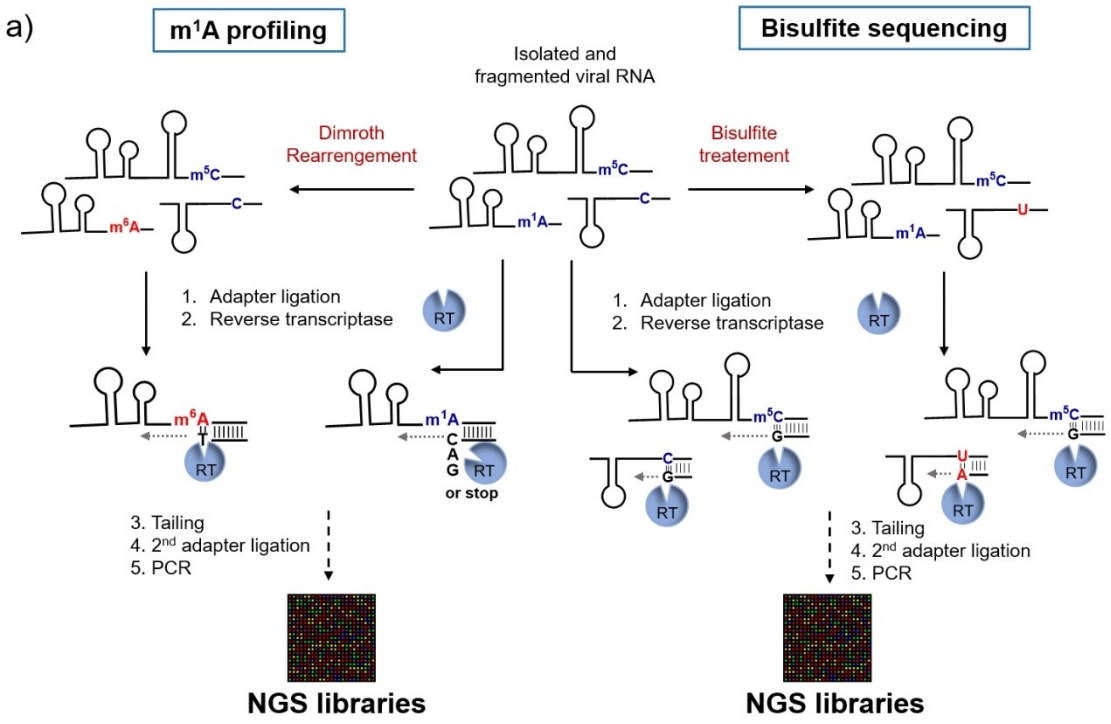

b)

	tRNA in SBV	tRNA in DWV	Bee – codon usage
1.	Lys CTT	Gly GCC-1	Glu GAA
2.	Gly GCC-1	Asp GTC	Lys AAA
3.	Lys TTT	Lys TTT	Asn AAT
4.	Asp GTC	Glu CTC	Asp GAT

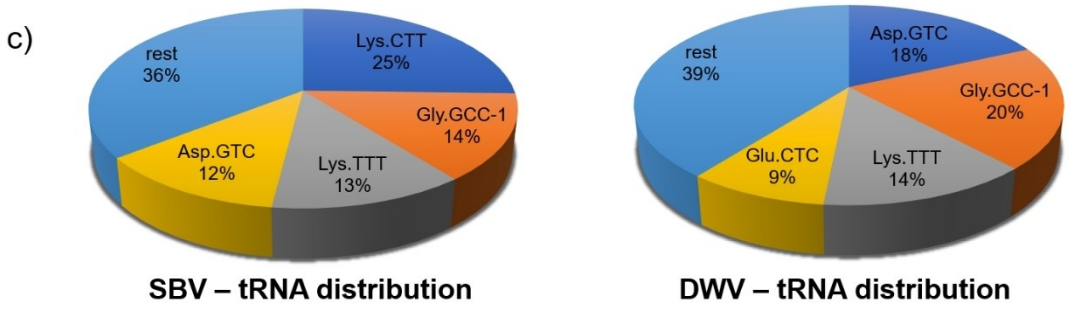

Figure 2. Detection of m^1A and m^5C position in RNA isolated from virions. a) Scheme of m^1A profiling and bisulfite sequencing applied on isolated RNA. b) Table of the detected tRNAs in SBV, DWV and honeybee codon usage. The blue color represents the tRNA that is also among the most used one in host organism. c) The ratio of co-packed tRNAs in SBV (detected in 6 samples) and DWV (detected in 2 samples).

Northern blot analysis of RNA from virions

We also analyzed RNA isolated from honeybee pupae and from SBV and DWV by Northern blots with ^{32}P labeled probes for 3′ and 5′ ends and for central region of $tRNA^{GlyGCC-1}$, $tRNA^{AspGTC}$, $tRNA^{LysTTT}$, $tRNA^{LysCTT}$ and $tRNA^{GluCTC}$. Surprisingly, we observed full length tRNAs in honeybee RNA but not in RNA from both viruses. Viruses contained only short fragments of these tRNAs. We prepared RNA ladder with $tRNA^{LysTTT}$ sequence of various size (21, 38 and 75 nt). The size of 3′ end fragments is around 38 nt. We were not able to detect 5′ end tRNA fragment of $tRNA^{AspGTC}$ but other 5′ tRNA fragments from $tRNA^{GlyGCC-1}$, $tRNA^{LysTTT}$, $tRNA^{LysCTT}$ and $tRNA^{GluCTC}$ were observed (Figure 3a, b). The size of the 5′ end tRNA fragments is comparable or shorter than 3′ tRNA fragments (Figure 3c). As we did not observe such tRNA fragments in the host organism, viruses probably trigger

© 2022 The Authors. ChemBioChem published by Wiley-VCH GmbH

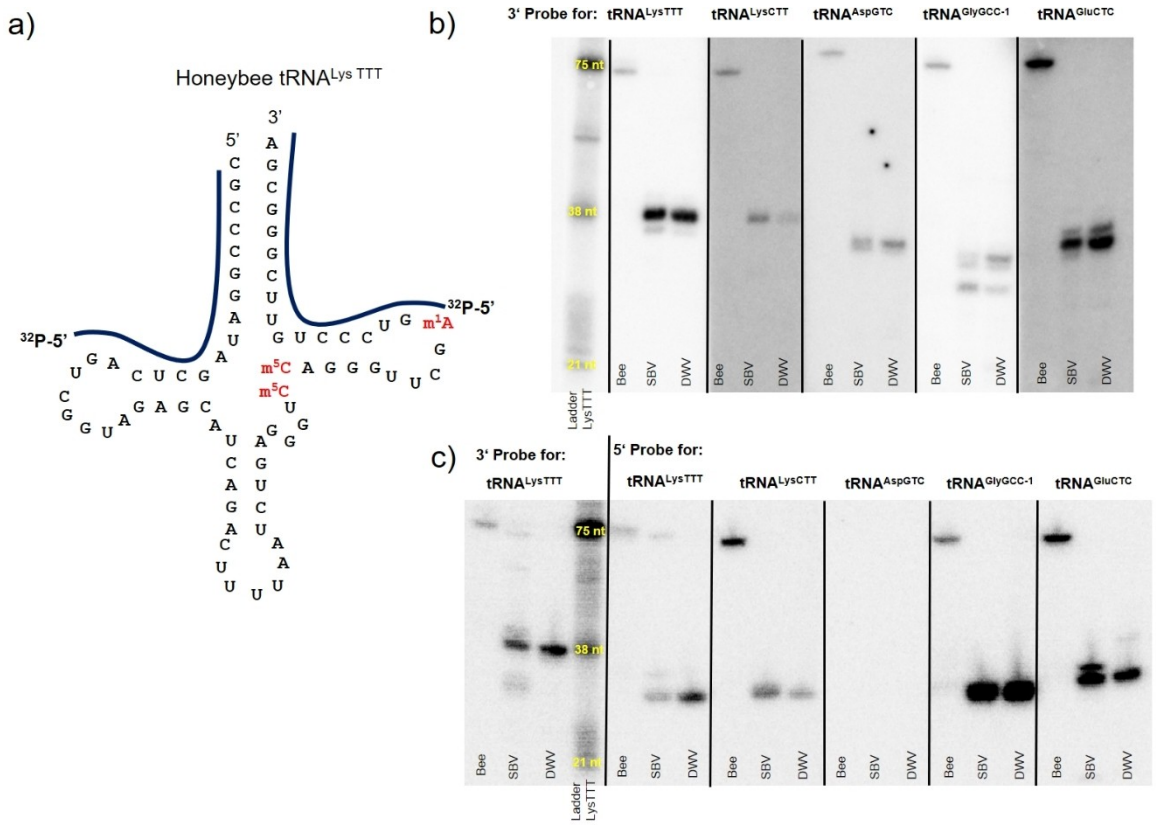

Figure 3. Detection of tRNAs in RNA isolated from Honeybee, SBV and DWV. a) Structure of Honeybee $tRNA^{Lys TTT}$. b) Northern blot analysis of isolated RNA and in vitro prepared RNA ladder with ^{32}P labeled probes for 3′ end of $tRNA^{LysTTT}$, $tRNA^{LysCTT}$, $tRNA^{AspGTC}$, $tRNA^{GlyGCC-1}$ and $tRNA^{GluCTC}$. c) Northern blot analysis of isolated RNA and in vitro prepared RNA ladder with ^{32}P labeled probes for 3′ end of $tRNA^{LysTTT}$ and 5′ end of $tRNA^{LysTTT}$, $tRNA^{LysCTT}$, $tRNA^{AspGTC}$, $tRNA^{GlyGCC-1}$ and $tRNA^{GluCTC}$.(Experiments were performed in triplicate).

the formation of these tRNA fragments and/or selectively co-pack these tRNA fragments in their particles.

Discussion

The current pandemic teaches us that the viruses represent the major threat to human populations and that we do not have available any general antivirotic useful in such situation. As we cannot presume, what other type of virus can threaten our society in future, it is necessary to learn as much as possible about virions composition and virus life cycle, in general.

Recently established epitranscriptomic field[18] focuses on mRNA modifications. The major challenge in the identification of new RNA modifications lies in the purification of cellular mRNA. Usually the most abundant tRNAs and rRNAs contaminate mRNA and their typical RNA modifications can be misinterpreted as originating from mRNA. In our search for new types of mRNA modifications, we identified viruses from *Picornavirales* order as the most suitable model systems. Until now, it was believed that the virions of these viruses contain solely genomic RNA, which they also use as mRNA. Therefore, the RNA purified from virions of *Picornavirales* should not contain any cellular RNA contamination. As RNA modifications help to virus to avoid the innate immune response of host organism and stabilize the viral RNA,[6] we presumed that discovery of some new RNA modifications in genomic RNA from *Picornavirales*, would help us to understand better virus life cycle. For our study, we choose four representatives from the *Picornavirales* order: insect iflaviridae (SBV and DWV) and human picornaviridae (E18 and RV2). We isolated RNA from pure virions and digested it into form of nucleosides. The mixtures of nucleosides were analyzed by LC–MS and compared with external standards of nucleosides. Surprisingly, we observed wide range of methylated nucleosides in the RNA isolated from SBV and DWV. The human viruses contained only low amount of 2′-O-methylated nucleosides and m^6A, which was recently detected also in enterovirus 71.[7]

To determine the exact position of m^1A and m^5C in viral RNA, we prepared RNA-seq libraries mapping m^1A and m^5C (bisulfite sequencing). To our surprise, we identified certain types of tRNAs in both viral samples. We were also able to identify the exact positions of m^1A in and m^5C in these co-packed tRNAs. The presence of these modifications was not conclusively confirmed in viral genomic RNA by our methods. This suggests that all the detected RNA modifications rather come from co-packed tRNAs. Moreover, in the light of the recent findings that e.g. m^1A is not present in human mRNA,[19]

© 2022 The Authors. ChemBioChem published by Wiley-VCH GmbH

our findings confirms the latest theories that mRNA is not so heavily modified as it was expected. Thus the viral genomic and mRNA will not contain wide range of modifications.[6] As we observed significant drops in tRNA reads (RNA-seq data), which are usually caused by sterically demanding modifications in close proximity of anticodon loop, we searched for three types of A modifications: t^6A, mS^2t^6A and i^6A, by LC–MS analysis. We confirmed the presence of all three modifications in RNA isolated from both viruses. This finding again confirms our theory that majority of detected modifications come from the co-packed tRNAs.

We also compared the types of co-packed tRNAs with codon-usage of honeybees to see whether these tRNAs that are the most abundant in host organism are also statistically co-packed in viral particle. Remarkably, the co-packed tRNAs do not correspond to ones most used by the host organism with only one exception – $tRNA^{LysTTT}$. In RNA isolate from virions from SBV, we identified four types of tRNAs: $tRNA^{LysCTT}$, $tRNA^{GlyGCC-1}$, $tRNA^{LysTTT}$ and $tRNA^{AspGTC}$ and from DWV, we identified beside $tRNA^{GlyGCC-1}$, $tRNA^{LysTTT}$ and $tRNA^{AspGTC}$ also $tRNA^{GluCTC}$. In both cases, these four types of tRNAs represent approx. 60% of all the tRNA pool in the viral particle. Other tRNAs were packed rather randomly. Surprisingly, the types of co-packed tRNAs in iflaviruses ($tRNA^{LysCTT}$, $tRNA^{LysTTT}$ and $tRNA^{AspGTC}$) are typical tRNA co-packed also by human retrovirus HIV-1, where $tRNA^{LysTTT}$ serves as primer for reverse transcription.[20] The role of the other tRNAs in HIV-1 viral particle is not well understood. It was suggested that other non-complemental tRNA may contribute to retroviral replication by shielding the membrane binding surface of the HIV matrix protein domain from the interactions with intracellular membranes before the Gag protein reaches the cellular membrane.[13d,21] Another hypothesis proposes that these tRNAs assist in HIV-1 nuclear transport[22] or that HIV-1 changes the host tRNA pool to enrich those tRNAs encoded in A-rich HIV genome.[23] As viruses from the order *Picornavirales* do not encode for Gag protein and their genomes are not transported into or out of nucleus, we cannot apply the retroviral explanation on them.

The main difference between packed tRNAs by retroviruses and *Picornavirales* is their size. While we detected full matured tRNAs in HIV-1,[13a] SBV and DWV contained 3′ and 5′ tRNA fragments. The production of such tRNA fragments was described under stress conditions and viral infection.[24] Particularly, it was shown that infection by respiratory syncytial virus (RSV, -ssRNA virus) leads to generation of 3′ and 5′ tRNA fragments.[25] 5′ tRNA fragments generated from $tRNA^{GlyCCC}$ and $tRNA^{LysCTT}$ promote RSV replication.[24] While part of 5′ tRNA fragment generated from $tRNA^{GluCTC}$ recognizes 3′-UTR of anti-RSV protein – apoliprotein E receptor 2 and suppress its expression.[26] 3′ end tRNA fragments generated from Proline tRNA were also detected in virus particles of human T-cell leukemia virus type 1, where they serve as primers for reverse transcriptase.[27] So far, the tRNA fragments have not been detected in +ssRNA viral particles. Nevertheless, our data together with previously reported tRNA fragments in other types of viruses suggest that the role of tRNA fragments can be quite general and that they may enhance viral replication or suppress antiviral response of host organism. The further studies will be necessary to explain this phenomenon and reveal real function of the co-packed tRNA fragments. For this purposes, model production of the insect viruses in tissue cell cultures will have to be established to allow functional experiments.

Recently, it was shown that double-stranded RNA regions from Flock House Virus genomic RNA were interacting with the capsid protein.[28] The disruption of these structures by mutations resulted in changes in viral replication, propagation, and packaging. The presence of D and L loops of tRNA fragments may be favored by the capsid proteins of iflaviruses and thus lead to co-packing of these host RNAs. The fact that tRNA fragments and not full tRNA are co-packed can be explained by steric reasons.

In summary, we discovered that some insects iflaviruses co-pack host cellular tRNA fragments. Till now, it was believed that *Picornavirales* virions contain only viral genomic RNA. This is the first evidence, confirmed by LC–MS, RNA-seq experiments and Northern blot analysis that *Picornavirales* also pack cellular tRNA fragments. The packing of tRNA fragments is not random or dependent on intracellular concentrations of tRNAs, but it is selective and only tRNA fragments from certain types e.g. $tRNA^{LysCTT}$, $tRNA^{LysTTT}$ and $tRNA^{AspGTC}$ are present in virions. Very interesting is finding that these types of tRNAs or fragments are also co-packed by virions of retroviruses such as HIV-1 or in RSV virions.

Experimental Section

Production and purification of honeybee viruses

SBV and DWV were purified as described previously.[12b,29] Briefly: one hundred experimentally infected honeybee pupae were homogenized using a Dounce homogenizer (piston-wall distance 0.075 mm) in 50 mL of phosphate buffered saline (PBS) on ice. The extract was centrifuged at 15,000×*g* for 30 min at 10 °C. The pellet was discarded, and the supernatant was ultracentrifuged at 150,000×*g* for 3 h in a Ti50.2 fixed-angle rotor (Beckman-Coulter) at 10 °C. The resulting pellet was resuspended in PBS in a final volume of 10 mL. $MgCl_2$ was added to a final concentration of 5 mM as well as 20 μg/mL of DNase I and 20 μg/mL of RNase. The solution was incubated at room temperature for 30 min and centrifuged for 15 min at 5,500 *g* at room temperature. The resulting supernatant was loaded onto 0.6 g/mL CsCl in PBS and centrifuged for 16 h at 30,000 rpm in an SW41 swinging-bucket rotor at 10 °C (Beckman-Coulter). Virus bands were collected by the gentle piercing of ultracentrifuge tubes with an 18-gauge needle. The viruses were buffer-exchanged to PBS and concentrated using centrifuge filter units with a 100-kDa molecular mass cutoff.

Production and purification of human viruses

Echovirus 18 (strain METCALF, obtained from ATCC-VR-852TM) was propagated in immortalized African green monkey kidney (GMK, 84113001 Sigma) cells cultivated in Dulbecco's modified Eagle's medium enriched with 10% fetal bovine serum. RV2 (strain HGP, ATCC-482) was propagated in HeLa (ATCC-CCL2) cells cultivated in Dulbecco's modified Eagle's medium enriched with 10% fetal bovine serum. For virus preparation, 50 tissue culture dishes with a

© 2022 The Authors. ChemBioChem published by Wiley-VCH GmbH

diameter of 150 mm of cells grown to 100% confluence were infected with a multiplicity of infection of 0.01. The infection was allowed to proceed for 2–3 days, at which point more than 90% of the cells exhibited a cytopathic effect. The cell media were harvested, and any remaining attached cells were removed from the dishes using cell scrapers. The cell suspension was centrifuged at 15,000×g in a Beckman Coulter Allegra 25R centrifuge, rotor A-10 at 10 °C for 30 min. The resulting pellet was resuspended in 10 mL of PBS. The solution was subjected to three rounds of freeze-thawing by transfer between −80 °C and 37 °C and homogenized using a Dounce tissue grinder. Cell debris was separated from the supernatant by centrifugation at 3,100×g in a Beckman Coulter Allegra 25R centrifuge, rotor A-10, at 10 °C for 30 min. The resulting supernatant was added to the media from the infected cells. Virus particles were precipitated by the addition of PEG-8000 and NaCl to final concentrations of 12.5% (w/v) and 0.6 M, respectively, and incubation overnight at 10 °C with mild shaking. The precipitate was centrifuged at 15,000×g in a Beckman Coulter Allegra 25R centrifuge, rotor A-10, at 10 °C for 30 min. The white precipitate was resuspended in 12 mL of PBS. $MgCl_2$ was added to a final concentration of 5 mM, and the sample was subjected to DNAse (10 μg/mL final concentration) and RNAse (10 μg/mL final concentration) treatment for 30 min at ambient temperature. Subsequently, trypsin was added to a final concentration of 0.5 μg/mL, and the mixture was incubated at 37 °C for 10 min. EDTA at pH 9.5 was added to a final concentration of 15 mM and a non-ionic detergent, NP-40™ (SigmaAldrich Inc.), was added to a final concentration of 1%. The virus particles were pelleted through a 30% (w/v) sucrose cushion in PBS by centrifugation at 210,000×g in an Optima X80 ultracentrifuge using a Beckman Coulter™Ti 50.2 rotor at 10 °C for 2 hours. The pellet was resuspended in 1.5 mL of PBS and loaded onto a 60% (w/w) CsCl solution in PBS. The CsCl gradient was established by ultracentrifugation at 160,000×g in an Optima X80 ultracentrifuge using a Beckman Coulter™SW41Ti rotor at 10 °C for 18 h. The opaque band containing the virus was extracted with a 20-gauge needle mounted on a 5 ml disposable syringe. The virus was transferred into PBS by multiple rounds of buffer exchange using a centrifugal filter device with a 100-kDa molecular weight cutoff. The final concentration of virus particles was 2 mg/mL.

Recording of cryo-electron micrographs of virus samples

Virus suspension (3.5 μL at concentration 2 mg/mL) was applied onto holey carbon grids (Quantifoil R2/1, mesh 300; Quantifoil Micro Tools) and vitrified by plunging into liquid ethane using an FEI Vitrobot Mark IV. Grids with the vitrified sample were transferred to an FEI Titan Krios electron microscope operated at 300 kV aligned for parallel illumination in nanoprobe mode. The sample in the column of the microscope was kept at −196 °C. Images were recorded with a Falcon III direct electron detection camera under low-dose conditions (46 e−/Å2) with under focus values about 3 μm at a nominal magnification of 75,000, resulting in a pixel size of 1.07 Å/pixel.

RNA isolation

RNA from *Iflaviruses* (SBV and DWV) and human *Picornaviruses* E18 and RV2 was isolated by Zymo-Spin™ IIC Columns (Direct-zol™ RNA MiniPrep Plus, Zymo) according to the manufacturer's protocol. RNA from honeybee was isolated from the whole body using TRIzol reagent according to the manufacturer's protocol. The quality of RNA samples was checked by HS RNA ScreenTape (4200 TapeStation, Agilent, Figure SI 8). RNA samples were quantified by an RNA High Sensitivity Assay (Quibit 4 Fluorometer, Thermofisher).

RNA digestion and LC–MS analysis

Picornaviral RNA samples (1.-10 μg) were fully digested by Nuclease P1 (1 U/μg of RNA, Sigma-Aldrich). Reaction was performed in 50 mM ammonium acetate buffer (pH 4.5) at 37 °C for 1 hour. After addition of Calf Intestine Alkaline Phosphatase (CIP, 1 U/μg of RNA, New England BioLabs) and CutSmart buffer (final concentration 1×), the samples were incubated for another 1 hour at 37 °C. Digested RNA samples were diluted in 200 μL and purified over Microcon® – 10 kDa centrifugal filters (Merck). The flow-through was concentrated using a SpeedVac system to the volume of 20 μL for LC–MS analysis.

The separation of the digested RNA was performed on an LC system (I–Class, Waters) with a C18 column (Acquity UPLC® BEH C18 1.7 μm, Waters) at 40 °C in gradient of 0.1% (v/v) formic acid in water (A) and 0.1% (v/v) formic acid in acetonitrile (B. The gradient was 0–6 min, 100% A; 6–7.5 min, 100–99% A; 7.5–9.5 min, 99–94% A; 9.5–15 min, 94% A; 15–25 min, 94–50% A; 25–27 min, 50–20%; 27–29.5 min, 20% A; 29.5–30 min, 20–100% A; 30–40 min, 100% A. The flow rate was 0.05 mL/min. The autosampler cooled the samples to 8 °C. The LC system was coupled on-line to a mass spectrometer (Synapt G2, Waters) to acquire masses of nucleosides by electrospray ionization. Ions were scanned in a positive polarity mode over full-scan range of *m/z* 100–1200. The source parameters were as follows: capillary voltage, 3 kV; source temperature, 150 °C; sampling cone, 40; extraction cone, 5; desolvation temperature, 450 °C; desolvation gas flow, 600 L/h.

LC–MS data (chromatograms) were analyzed by software MassLynx V4.1. A mixture of nucleoside standards from each canonical and methylated nucleoside (A, m^1A, m^6A, Am; G, m^1G, m^2G, m^7G, Gm; C, m^3C, m^5C, Cm; U, m5 U, Um) were measured in ratio 100×canonical base: 1×methylated bases. Standard mixtures were injected on a column to compare the response of each nucleoside under defined ionization conditions. The mixture was measured in the technical triplicate. For each standard, an extracted ion chromatogram (XIC) was generated using a major fragment observed in its full scan spectrum (fragmentation occurs in the ion source). The chromatographic peaks in XICs were integrated. The standard peak area (area under the curve, AUC) was used to calculate the ionization efficiency ratio of the tested nucleosides.

The chromatographic peaks of the major fragments in XICs were integrated and the AUC was used *to* calculate the amount of each modification per 100 unmodified nucleosides (Figure 1b).

RNA sequencing library preparation

m^1A mapping: The first RNA-seq library was prepared from SBV isolated RNA by protocol described previously.[13a] Shortly, chemical fragmentation (metal-ion induced) was used to achieved size distribution of fragments from 50–200 nt. Samples were ethanol precipitated. To have a negative control, rearrangement of m^1A to m^6A was performed by alkali treatment. One-half of each sample was incubated with alkaline buffer (50 mM Na_2CO_3, 2 mM EDTA, pH 10.4) for 1 h at 60 °C and purified by RNA Clean & Concentrator columns (Zymo). After adaptor ligation and couple of purification steps reverse transcriptase (RT) was used. To confirm the position of m^1A two RTs (SuperScript™ III reverse transcriptase and TGIRT™ reverse transcriptase) were used. Each should show different pattern (misincorporation or break) when meet m^1A. RNA was degraded and after cDNA tailing and barcode-labeling samples were submitted for sequencing on Ion Torrent platform.

Bisulfite sequencing: For second library (SBV, DWV) was used similar protocol but additional step of bisulfite treatment was added. After chemical fragmentation, one half of SBV and DWV

© 2022 The Authors. ChemBioChem published by Wiley-VCH GmbH

samples was used for bisulfite conversion. This was done by EZ RNA Methylation™ Kit (Zymo Res. Com.) according to the manufacturer's protocol. The quality of RNA samples was checked by HS RNA ScreenTape (4200 TapeStation, Agilent). RNA samples were quantified by an RNA High Sensitivity Assay (Quibit 4 Fluorometer, Thermofisher). Samples were purified and concentrated by ethanol precipitation and submitted for sequencing on Ion Torrent platform. Only SuperScript™ III reverse transcriptase was used to prepare this library.

Bioinformatic analysis

After quality control performed by FastQC (https://www.bioinformatics.babraham.ac.uk/projects/fastqc) libraries were split by fastx toolkit (http://hannonlab.cshl.edu/fastx_toolkit/index.html) and all barcodes and technical sequences were trimmed by combination of trimmomatic[30] and cutadapt[31] software. Sequences longer than 20bp were mapped using bwa aligner v0.7.17.[32] We mapped reads to modified SBV (GeneBank accession NC_002066.1) and DWV (NC_004830.2) viral genomes which represent particular strains used in experiments. Honeybee tRNA from the literature were clustered and only one representative for each group was used for mapping. Detection and statistical evaluation of misincorporations, insertions, deletions or premature ends were done in our own software available at https://github.com/bioinfocz/rnamod under MIT license. Program uses a SAM file generated by bwa as an input and from CIGAR string field detects differences and performs paired t-test between sample and control, then creates graphical and textual output of coverage and significant positions. Parameters for significant positions used for misincorporation and premature end were: (coverage $>$ 100 && err $>$ 0.4) $||$ (coverage $>$ 100 && p-value $<$ 0.1 && err $>$ 0.1); for insertion or deletion simply err $>$ 0.3.[33]

RNA ladder preparation

DNA templates for 21, 38 and 75 nt long RNA ladder (Table SI 12) were annealed in annealing buffer (10 mM Tris, 50 mM NaCl, 1 mM EDTA pH 7,8). In vitro transcription was performed as described[34] in a 50 μL mixture (0.2 μM of template DNA, 1 mM of each NTP (NEB), 5% dimethyl sulfoxide (DMSO, NEB), 0.12% triton X-100 (Sigma-Aldrich), 10 mM dithiothreitol (DTT), 4.8 mM MgCl2 (Sigma-Aldrich), 1×reaction buffer for T7 RNAP (NEB) and 125 units of T7 RNAP (New England BioLabs, NEB)). The mixture was incubated for 2 h at 37 °C. The DNA template was digested by DNAse I (NEB) at 37 °C for 45 min and the enzyme was heat inactivated at 75 °C for 10 min. Samples were purified using Clean and concentrator (Zymo), mixed in ratio 1 : 1 : 1 and 3 μL were loaded on the gel.

Northern blot analysis

Denaturing polyacrylamide gel (12.5%) was prepared from Rotiphorese gel (Carl Roth) in 1×TBE buffer. The polymerized gel was pre-run at 600 V for 30 min in 1×TBE buffer. All RNA samples (500 ng of honeybee RNA/well, 5000 ng of SBV RNA/well, 1200 ng or 5000 ng of DWV RNA/well) were denatured for 15 min at 55 °C and loaded into the gel wells. The gel was run at 600 V for 1–2 hours and then blotted onto a charged nylon membrane (Amersham Hybond-N+; GE Healthcare) by capillary transfer in 20×SSC buffer (3 M NaCl, 0.3 M trisodium citrate, pH adjusted to 7.0) overnight. The membrane was crosslinked twice on a default setting (120 mJ, 30 s) using electronic ultraviolet crosslinker (Ultralum). The crosslinked membrane was hybridized with 10 mL of Church buffer (70 mM NaH_2PO_4, 180 mM Na_2HPO_4, 7% SDS, 1% BSA, 1 mM EDTA, pH 7.2) at 45 °C for 1 h using a ProBlot hybridization oven (Labnet). Meanwhile, 2.5 μL of 100 μM tRNA probe (Table SI 12) was end-labelled by 10 U T4 Polynucleotide Kinase (Thermofisher Scientific) and 1 μL of γ-^{32}P-ATP (3.3 μM, 10 μCi/μL; Hartmann analytic) in 10 μL of supplemented kinase buffer at 37 °C for 30 min. The enzyme was inactivated at 65 °C for 5 min and the probe was purified from unincorporated nucleotides using mini Quick Spin RNA columns (Roche) according to the manufacturer's instructions. The probe was added to the membrane in 10 mL of fresh Church buffer and hybridized at 45 °C, overnight. The membranes were washed twice for 10 min each with low stringency buffer (2×SSC+0.1% SDS) and once with high stringency buffer (0.1×SSC+0.1% SDS), all at 45 °C. The membranes were sealed in foil, incubated with phosphor imaging plate (GE healthcare) and scanned using Typhoon FLA 9500 (GE Healthcare).

Acknowledgement

The work was supported from Ministry of Education, Youth and Sports (Czech Republic), program ERC CZ (LL1603). The bioinformatics part of the work including access to computing and storage facilities was supported by the ELIXIR CZ research infrastructure project (MEYS Grant No: LM2018131). The primary data of the RNA-seq experiments are accessible at https://www.ebi.ac.uk/ena/browser/home under the project accession number PRJEB53666.

Conflict of Interest

The authors declare no conflict of interest.

Data Availability Statement

The data that support the findings of this study are available from the corresponding author upon reasonable request.

Keywords: human rhinovirus type 2 · human Echovirus 18 · LC–MS · *Picornavirales* · RNA methylation · tRNA fragments

[1] B. Bagiński, E. Purta, P. Piątkowski, P. Boccaletto, T. K. Wirecki, M. A. Machnicka, J. M. Bujnicki, V. de Crécy-Lagard, P. A. Limbach, R. Ross, A. Kotter, M. Helm, *Nucleic Acids Res.* **2017**, *46*, D303–D307.
[2] a) K. D. Meyer, Y. Saletore, P. Zumbo, O. Elemento, C. E. Mason, S. R. Jaffrey, *Cell* **2012**, *149*, 1635–1646; b) D. Dominissini, S. Moshitch-Moshkovitz, S. Schwartz, M. Salmon-Divon, L. Ungar, S. Osenberg, K. Cesarkas, J. Jacob-Hirsch, N. Amariglio, M. Kupiec, R. Sorek, G. Rechavi, *Nature* **2012**, *485*, 201.
[3] K. Slama, A. Galliot, F. Weichmann, J. Hertler, R. Feederle, G. Meister, M. Helm, *Methods* **2019**, *156*, 102–109.
[4] F. Di Serio, E. M. Torchetti, J. A. Daròs, B. Navarro, *Viruses* **2019**, *11*, 357.
[5] a) K. Borland, J. Diesend, T. Ito-Kureha, V. Heissmeyer, C. Hammann, A. H. Buck, S. Michalakis, S. Kellner, *Genes* **2019**, *10*, 26; b) V. F. Reichle, S. Kaiser, M. Heiss, F. Hagelskamp, K. Borland, S. Kellner, *Methods* **2019**, *156*, 91–101; c) M. Helm, Y. Motorin, *Nat. Rev. Genet.* **2017**, *18*, 275; d) M. Helm, J. D. Alfonzo, *Chem. Biol.* **2014**, *21*, 174–185.
[6] J. F. Potužník, H. Cahová, *mBio* **2020**, *11*, e02131–02120.
[7] H. Hao, S. Hao, H. Chen, Z. Chen, Y. Zhang, J. Wang, H. Wang, B. Zhang, J. Qiu, F. Deng, W. Guan, *Nucleic Acids Res.* **2018**, *47*, 362–374.
[8] A. M. Fendrick, A. S. Monto, B. Nightengale, M. Sarnes, *Archives Int. Med.* **2003**, *163*, 487–494.

© 2022 The Authors. ChemBioChem published by Wiley-VCH GmbH

[9] H. Zhang, Y. Zhao, H. Liu, H. Sun, X. Huang, Z. Yang, S. Ma, *Sci. Rep.* **2017**, *7*, 8448.
[10] L. M. Brutscher, A. J. McMenamin, M. L. Flenniken, *PLoS Pathog.* **2016**, *12*, e1005757.
[11] S. G. Potts, J. C. Biesmeijer, C. Kremen, P. Neumann, O. Schweiger, W. E. Kunin, *Trends Ecol. Evol.* **2010**, *25*, 345–353.
[12] a) G. Lanzi, J. R. de Miranda, M. B. Boniotti, C. E. Cameron, A. Lavazza, L. Capucci, S. M. Camazine, C. Rossi, *J. Virol.* **2006**, *80*, 4998–5009; b) K. Skubnik, J. Novacek, T. Fuzik, A. Pridal, R. J. Paxton, P. Plevka, *Proc. Natl. Acad. Sci. USA* **2017**, *114*, 3210–3215; c) J. Dong, R. Guo, M. Huang, D. Wang, J. Huang, *J. Asia-Pacific Entomol.* **2020**, *23*, 76–81; d) M. Procházková, T. Füzik, K. Škubník, J. Moravcová, Z. Ubiparip, A. Přidal, P. Plevka, *Proc. Natl. Acad. Sci. USA* **2018**, *115*, 7759–7764.
[13] a) A. Šimonová, B. Svojanovská, J. Trylčová, M. Hubálek, O. Moravčík, M. Zavřel, M. Pávová, J. Hodek, J. Weber, J. Cvačka, J. Pačes, H. Cahová, *Sci. Rep.* **2019**, *9*, 8697; b) A. Telesnitsky, S. Wolin, *Viruses* **2016**, *8*, 235; c) M. J. Eckwahl, H. Arnion, S. Kharytonchyk, T. Zang, P. D. Bieniasz, A. Telesnitsky, S. L. Wolin, *RNA* **2016**, *22*, 1228–1238; d) M. J. Eckwahl, A. Telesnitsky, S. L. Wolin, *mBio* **2016**, *7*, e02025–15; e) M. J. Eckwahl, S. Sim, D. Smith, A. Telesnitsky, S. L. Wolin, *Genes Dev.* **2015**, *29*, 646–657.
[14] S. K. Behura, M. Stanke, C. A. Desjardins, J. H. Werren, D. W. Severson, *Insect Mol. Biol.* **2010**, *19*, 49–58.
[15] B. A. Elliott, H.-T. Ho, S. V. Ranganathan, S. Vangaveti, O. Ilkayeva, H. Abou Assi, A. K. Choi, P. F. Agris, C. L. Holley, *Nat. Commun.* **2019**, *10*, 3401.
[16] R. Hauenschild, L. Tserovski, K. Schmid, K. Thüring, M. L. Winz, S. Sharma, K. D. Entian, L. Wacheul, D. L. Lafontaine, J. Anderson, J. Alfonzo, A. Hildebrandt, A. Jäschke, Y. Motorin, M. Helm, *Nucleic Acids Res.* **2015**, *43*, 9950–9964.
[17] P. Boccaletto, M. A. Machnicka, E. Purta, P. Piątkowski, B. Bagiński, T. K. Wirecki, V. de Crécy-Lagard, R. Ross, P. A. Limbach, A. Kotter, M. Helm, J. M. Bujnicki, *Nucleic Acids Res.* **2017**, *46*, D303-D307.
[18] K. D. Meyer, S. R. Jaffrey, *Nat. Rev. Mol. Cell Biol.* **2014**, *15*, 313–326.
[19] M. Safra, A. Sas-Chen, R. Nir, R. Winkler, A. Nachshon, D. Bar-Yaacov, M. Erlacher, W. Rossmanith, N. Stern-Ginossar, S. Schwartz, *Nature* **2017**, *551*, 251.
[20] L. Kleiman, *IUBMB Life* **2002**, *53*, 107–114.
[21] S. B. Kutluay, T. Zang, D. Blanco-Melo, C. Powell, D. Jannain, M. Errando, P. D. Bieniasz, *Cell* **2014**, *159*, 1096–1109.
[22] L. Zaitseva, R. Myers, A. Fassati, *PLoS Biol.* **2006**, *4*, e332.
[23] M. Pavon-Eternod, M. Wei, T. Pan, L. Kleiman, *RNA* **2010**, *16*, 267–273.
[24] X. Yu, Y. Xie, S. Zhang, X. Song, B. Xiao, Z. Yan, *Theranostics* **2021**, *11*, 461–469.
[25] J. Zhou, S. Liu, Y. Chen, Y. Fu, A. J. Silver, M. S. Hill, I. Lee, Y. S. Lee, X. Bao, *J. Gen. Virol.* **2017**, *98*, 1600–1610.
[26] J. Deng, R. N. Ptashkin, Y. Chen, Z. Cheng, G. Liu, T. Phan, X. Deng, J. Zhou, I. Lee, Y. S. Lee, X. Bao, *Mol. Ther.* **2015**, *23*, 1622–1629.
[27] K. Ruggero, A. Guffanti, A. Corradin, V. K. Sharma, G. De Bellis, G. Corti, A. Grassi, P. Zanovello, V. Bronte, V. Ciminale, D. M. D'Agostino, *J. Virol.* **2014**, *88*, 3612–3622.
[28] Y. Zhou, A. Routh, *Nucleic Acids Res.* **2020**, *48*, e12-e12.
[29] a) M. Prochazkova, K. Skubnik, T. Fuzik, L. Mukhamedova, A. Pridal, P. Plevka, *Curr. Opin. Virol.* **2020**, *45*, 17–24; b) S. Kalynych, A. Pridal, L. Palkova, Y. Levdansky, J. R. de Miranda, P. Plevka, *J. Virol.* **2016**, *90*, 7444–7455.
[30] A. M. Bolger, M. Lohse, B. Usadel, *Bioinformatics* **2014**, *30*, 2114–2120.
[31] M. Martin, *EMBnet. J.* **2011**, *17*, 3.
[32] H. Li, R. Durbin, *Bioinformatics* **2009**, *25*, 1754–1760.
[33] J. P. Didion, M. Martin, F. S. Collins, *PeerJ* **2017**, *5*, e3720.
[34] F. Huang, *Nucleic Acids Res.* **2003**, *31*, e8–e8.

Manuscript received: May 17, 2022
Revised manuscript received: June 30, 2022
Accepted manuscript online: June 30, 2022
Version of record online: July 21, 2022

© 2022 The Authors. ChemBioChem published by Wiley-VCH GmbH